

# Series expansion for a stochastic sandpile

Jürgen F. Stilck<sup>1,\*</sup>, Ronald Dickman<sup>2,†</sup> and Ronaldo R. Vidigal<sup>2,‡</sup>

<sup>1</sup>*Departamento de Física, Universidade Federal Fluminense, Av. Litorânea s/n,  
24210-340*

*Niterói - Rio de Janeiro, Brasil*

<sup>2</sup>*Departamento de Física, ICEx, Universidade Federal de Minas Gerais,  
30123-970 Belo Horizonte - Minas Gerais, Brasil*

(February 7, 2020)

## Abstract

Using operator algebra, we extend the series for the activity density in a one-dimensional stochastic sandpile with fixed particle density  $p$ , the first terms of which were obtained via perturbation theory [R. Dickman and R. Vidigal, J. Phys. A **35**, 7269 (2002)]. The expansion is in powers of the time; the coefficients are polynomials in  $p$ . We devise an algorithm for evaluating expectations of operator products and extend the series to  $\mathcal{O}(t^{16})$ . Constructing Padé approximants to a suitably transformed series, we obtain predictions for the activity that compare well against simulations, in the supercritical regime.

PACS: 05.70.Ln, 02.50.Ga, 05.10.Gg, 05.40.-a

\*electronic address: jstilck@if.uff.br

†electronic address: dickman@fisica.ufmg.br

‡electronic address: rvidigal@dedalus.lcc.ufmg.br

## I. INTRODUCTION

Sandpiles with a strictly conserved particle density (so-called *fixed-energy sandpiles* or FES [1]), exhibit absorbing-state phase transitions [2–4], and have recently attracted much interest. Until now, most quantitative results for FES have been based on simulations [5–8], an important exception being the solution by Priezzhev *et al.* [9] of a directed, fixed-energy version of the Maslov-Zhang model [10], via the Bethe ansatz. It is therefore of great interest to develop theoretical approaches for FES.

Series analysis has proved to be one of the most accurate and reliable approaches to critical phenomena, in both equilibrium and nonequilibrium contexts [11–14]. Series expansion typically functions best in low-dimensional systems (because longer series can be derived), that is, for just those systems in which the renormalization group and expansion about an upper critical dimension  $d_c$  are less reliable. In the case of sandpiles, systematic epsilon expansions are as yet unavailable, and the value of  $d_c$  in fact remains controversial [15–17]. Simulation results suggest novel critical behavior in the one-dimensional FES, although conflicting critical exponent values have been reported [7,8,18,19], which may reflect finite-size effects. Series expansions, on the other hand, implicitly treat the infinite-size limit, and so provide important information, complementary to that afforded by simulations. In light of these observations, we believe it highly desirable to apply series methods to sandpile models.

This paper is one of a series analyzing a stochastic sandpile using operator methods. In an earlier work [20] a path-integral representation was developed and an expansion derived for the order parameter (activity density) in powers of time. While the path-integral formalism reveals interesting features of the model, and may be applied in any number of dimensions, the complexity of the diagrammatic expansion limits the number of terms that can be obtained. (In Ref. [20] terms up to  $\mathcal{O}(t^5)$  are reported.) In this paper we employ a different approach, which permits us to extend the series for the one-dimensional case considerably. After casting the master equation for the sandpile in terms of an operator formalism, we analyze the direct expansion of its (formal) solution, leading to an algorithm for generating the series coefficients.

We consider Manna’s stochastic sandpile in its fixed-energy (particle-conserving) version [7,20–22]. The configuration is specified by the occupation number  $n$  at each site; sites with  $n \geq 2$  are said to be *active*, and have a positive rate of *toppling*. When a site topples, it loses exactly two particles (“grains of sand”), which move randomly and independently to nearest-neighbor (NN) sites. (Any configuration devoid of active sites is *absorbing*, i.e., no further evolution of the system is possible once such a configuration is reached.) In this work, as in Ref. [20], we adopt a toppling rate of  $n(n-1)$  at a site having  $n$  particles, which leads us to define the order parameter as  $\rho = \langle n(n-1) \rangle$ . While this choice of rate represents a slight departure from the

usual definition (in which all active sites have the same toppling rate), it leads to a much simpler evolution operator, and should yield the same scaling properties [20]. Preliminary simulation results [23] indicate that in one dimension the model exhibits a continuous phase transition at  $p_c=0.9493$ .

In the following section we define the model and review the operator formalism introduced in Ref. [20]. This is followed in Sec. III by an analysis leading to an expansion in terms of so-called reduced commutators. Implementation of the expansion in a computational algorithm is described in Sec. IV. Then in Sec. V we report numerical results of the series analysis. A summary and discussion is provided in Sec. VI.

## II. MODEL

As discussed in Ref. [20], the master equation for this model may be written in the form

$$\frac{d|\Psi\rangle}{dt} = L|\Psi\rangle, \quad (1)$$

where

$$|\Psi\rangle = \sum_{\{n_i\}} p(\{n_i\}, t) |\{n_i\}\rangle,$$

is the probability distribution, and the evolution operator takes the form,

$$L = \sum_i \left[ \frac{1}{4} (\pi_{i-1} + \pi_{i+1})^2 - \pi_i^2 \right] a_i^2 \equiv \sum_i L_i. \quad (2)$$

Here  $a_i$  and  $\pi_i$  are, respectively, annihilation and creation operators associated with site  $i$ , defined via

$$a_i |n_i\rangle = n_i |n_i - 1\rangle$$

and

$$\pi_i |n_i\rangle = |n_i + 1\rangle.$$

The formal solution of the master equation is  $|\Psi(t)\rangle = e^{tL}|\Psi(0)\rangle$ ; that for the activity density is:

$$\rho(t) = \langle |a_0^2 e^{tL} |\Psi(0)\rangle. \quad (3)$$

Here we have introduced the notation:

$$\langle | \equiv \sum_{\{n\}} \langle \{n\} | \quad (4)$$

for the projection onto all possible states; thus normalization reads:  $\langle | \Psi \rangle = 1$ . We consider a uniform Poisson-product initial distribution. Letting  $p_n = e^{-p} p^n / n!$ , and using  $|P\rangle_i = \sum_{n_i} p_{n_i} |n\rangle_i$  to denote a Poisson distribution at site  $i$ , we have,

$$|\Psi(0)\rangle = \prod_j |P\rangle_j . \quad (5)$$

We shall expand equation (3) for the activity density in powers of  $t$ .

### III. OPERATOR ALGEBRA

To begin we note some basic properties of operators  $a_j$ ,  $\pi_j$  and  $L_j$ :

$$a_j^n |P\rangle_j = p^n |P\rangle_j \quad (6)$$

$$\langle | \pi_j = \langle | \quad (7)$$

$$\langle | L_i = 0 \quad (8)$$

$$[a_i, \pi_j] = \delta_{i,j} \quad (9)$$

$$[L_i, L_j] = [a_i, L_j] = 0 \quad \text{for } |i - j| > 1 . \quad (10)$$

The second relation expresses the fact that the creation operator conserves the normalization of any state, while the third shows that  $L_i$  conserves probability, as it must.

The coefficient of  $t^n/n!$  in the expansion of the activity is:

$$\sum_{\mathcal{S}} \langle | a_0^2 L_{s_1} L_{s_2} \dots L_{s_n} | P \rangle , \quad (11)$$

where the sum is over all sequences  $\mathcal{S}$  of sites  $s_0 \equiv 0, s_1, \dots, s_n$  with  $|s_1| \leq 1$ , and  $s_{j+1} \in \{s_{j,min} - 1, \dots, s_{j,max} + 1\}$ , for  $j \geq 1$ , where  $s_{j,min} = \min\{s_0, \dots, s_j\}$ , and  $s_{j,max}$  is the maximum of this set. The restriction on sequences follows from equations (8)

and (10); if the condition were violated, it would be possible to move one of the  $L_j$  to the left of all other operators, yielding a result of zero.

Our strategy for evaluating  $\rho_S$  is to commute each  $L_j$  to the left of  $a_0^2$ . The first step replaces  $a_0^2 L_{s_1}$  by its commutator, due to equation (8). If we write this commutator in *normal order*, that is, with all creation operators  $\pi_j$  to the left of all annihilation operators, then the  $\pi$ 's may be replaced by 1, by equation (7). Thus,

$$\langle |a_0^2 L_j = \langle |[a_0^2, L_j]_R, \quad (12)$$

where the subscript  $R$  denotes a *reduced commutator*, that is, the commutator in normal order, with all  $\pi$ 's replaced by unity. Evidently  $[a_0^2, L_j]_R$  involves only annihilation operators. The two nontrivial expressions of this kind are:

$$[a_0^2, L_0]_R = -2a_0^2 - 4a_0^3, \quad (13)$$

and

$$[a_0^2, L_1]_R = \frac{1}{2}a_1^2 + 2a_0a_1^2. \quad (14)$$

In the computational algorithm, discussed in some detail below, it is not necessary to generate the tree structure of sequences explicitly, since each monomial is processed separately and both translation and reflection symmetries may be used in the calculations of the contributions  $\rho_S$ . Evaluating the expectation of each term in  $\rho_S$  is trivial, because

$$\langle |a_{s_1}^{m_1} \dots a_{s_n}^{m_n} |P\rangle = p^M, \quad (15)$$

where  $M = \sum_j m_j$  is the number of annihilation operators, irrespective of which sites are involved.

It remains to find a general expression for the reduced commutator  $[F^{(j)}, L_k]_R$ . Since  $F^{(j)}$  is a linear combination of products of annihilation operators, and recalling that  $a_i$  and  $L_k$  commute if  $|i-k| > 1$ , we see that the problem reduces to evaluating

$$C(p, q, r) \equiv [a_{-1}^p a_0^q a_1^r, L_0]_R. \quad (16)$$

(Commutators involving  $L_j$  with  $j \neq 0$  are obtained using translation invariance.) It is straightforward to evaluate  $C(p, q, r)$  using the following identities. First we note that

$$[a_j^p, \pi_j] = p a_j^{p-1}, \quad (17)$$

as is readily shown by induction. Using this it is simple to show

$$[a_j^p, \pi_j^2]_R = p(p-1)a_j^{p-2} + 2pa_j^{p-1}, \quad (18)$$

and

$$[a_j^p, \pi_j^2 a_j^2]_R = p(p-1)a_j^p + 2pa_j^{p+1}. \quad (19)$$

Finally, we may use equation (17) to show that for  $i \neq j$ ,

$$[a_i^p a_j^r, \pi_i \pi_j]_R = pa_i^{p-1} a_j^r + ra_i^p a_j^{r-1} + pra_i^{p-1} a_j^{r-1}. \quad (20)$$

Applying these relations one readily finds:

$$\begin{aligned} C(p, q, r) = a_0^{q+2} & \left[ \frac{1}{4}p(p-1)a_{-1}^{p-2}a_1^r + \frac{1}{4}r(r-1)a_{-1}^p a_1^{r-2} \right. \\ & + \frac{1}{2}pra_{-1}^{p-1}a_1^{r-1} + pa_{-1}^{p-1}a_1^r + ra_{-1}^p a_1^{r-1} \Big] \\ & - qa_{-1}^p a_1^r [2a_0^{q+1} + (q-1)a_0^q]. \end{aligned} \quad (21)$$

Using this result, we can evaluate the reduced commutators in a computer algorithm.

#### IV. COMPUTATIONAL ALGORITHM

Let us discuss some details of the computer algorithm used to generate the series for the activity. We employ a recursive procedure to generate the contributions of order  $n+1$  on the basis of those of order  $n$ . From equation (3) and with a Poisson-product initial distribution defined in equation (5) we notice that

$$\frac{d\rho}{dt} = \langle |a_0^2 L e^{tL} | P \rangle = \langle |[a_0^2, L]_R e^{tL} | P \rangle = -\rho + \langle |(4a_0 a_1^2 - 4a_0^3) e^{tL} | P \rangle. \quad (22)$$

The last equality above may be understood using the reduced commutators (13) and (14). Using reflection symmetry, we have  $\langle |[a_0^2, L]_R e^{tL} | P \rangle = \langle |\{[a_0^2, L_0]_R + 2[a_0^2, L_1]_R\} e^{tL} | P \rangle$  and further simplification is provided by translation symmetry. The coefficient of  $t^n/n!$  in the expansion of the activity may be identified with  $C_n$ , where

$$C_n = \left. \frac{d^n \rho}{dt^n} \right|_{t=0}. \quad (23)$$

Using the procedure described above we obtain a recursion relation

$$C_{n+1} = -C_n + \langle |F_{n+1}|P \rangle, \quad (24)$$

where  $F_{n+1} = [F_n, L]$  and  $F_1 = 4a_0a_1^2 - 4a_0^3$ . To complete the algorithm, we have that  $C_0(0) = \rho(0) = \langle |a_0^2| \rangle = p^2$ , where relation (15) is used. An immediate consequence of these recursion relations is that the coefficient of  $p^2$  in the term of order  $n$  in  $t$  is given by  $(-1)^n$ , since each monomial in the functions  $F$  has at least three annihilation operators [24]. This was already shown in Ref. [20].

The calculations were done in two steps. Initially, the functions  $F$  were calculated up to order 12. Each monomial was represented by three integer variables: an eight-byte integer for the numerator of the coefficient, a four-byte integer for the denominator (which is always a power of 2), and another eight-byte integer to store the number of factors of each annihilation operator. Since all calculations are done in integer arithmetic, there are no roundoff errors. Using translation invariance, each monomial was put in a form such that the annihilation operator of lowest spatial index is  $a_0$ . The power  $m_i$  associated with each annihilation operator  $a_{s_i}$  (as in equation (15)) is stored in four bits of the eight-byte integer variable mentioned above. As each new monomial is generated, a search is performed for any existing term with the same set of powers; storing all powers in a single integer facilitates the search. As a consequence of equation (10), when the reduced commutator of a monomial with  $L$  is calculated, nonzero contributions may arise only from the commutator of the monomial with  $L_{-1}, L_0, L_1, \dots, L_{i+1}$ , where  $i$  is the largest index in the monomial. As is clear from equation (21), each of these commutators can give rise to up to seven new monomials. Thus, it is apparent that the number of monomials grows very rapidly as the order is increased; the function  $F_{12}$  involves 519 115 monomials. To go beyond order 12 it is necessary to handle integers larger than can be represented using eight bytes and to process monomials with more than 16 exponents, which can no longer be stored in a single 8-byte integer variable. In fact, at order 12 most of the processing time is used in the search procedure. Therefore, our results from order 13 to 16 were obtained processing the monomials in  $F_{12}$  one-by-one, generating all contributions from it at orders 13-16. In these calculations the numerators were represented by two eight-byte integers. The limiting order (16) is determined by the large number of new monomials generated; a single monomial in  $F_{15}$  may generate on the order of 40 monomials in  $F_{16}$ . The results presented here required about 170 hours of cpu time on an Athlon K7 1800 MHz computer.

It is convenient to write the expansion in the form:

$$\bar{\rho}(t) \equiv \frac{\rho(t)}{p^2} = \sum_n \frac{(-t)^n}{n!} \sum_{m=0}^{n-1} b_{n,m} p^m. \quad (25)$$

The series coefficients  $b_{n,m}$  are listed in Table I. In Ref. [20] it was shown that  $m \leq n-1$ , with

$$b_{n,n-1} = 2^{4n-1} \frac{(2n-1)!!}{(2n+2)!!}. \quad (26)$$

The coefficients reported in Table I satisfy this relation at each order, and agree with those derived (for  $n \leq 5$ ) using the path-integral formalism [20].

## V. ANALYSIS OF SERIES

The coefficients  $b_{n,m}/n!$  in the time series, equation (25), grow rapidly with  $n$ ; the rate of growth appears to be faster than exponential. This is evident from an analysis of

$$h_{n,m} \equiv \ln \left( \frac{b_{n,m}}{n!} \right) \quad (27)$$

To see if the  $h_{n,m}$  follow a systematic trend we analyze these quantities for a given  $q \equiv (m-1)/(n-2)$ . (For a fixed value of  $n$ , the  $h_{n,m}$  appear to trace out a smooth curve, so that  $h_n(q)$  for intermediate values of  $q$  can be estimated via interpolation.) As shown in figure 1,  $h_n(q)$  appears to grow faster than exponentially with  $n$ , away from the limits  $q = 0$  and  $q = 1$ . (Observe that for  $m = 0$ ,  $h_{m,n} \rightarrow -\infty$  as  $n \rightarrow \infty$  since  $b_{n,0} = 1$ , and similarly for  $m = n-1$ , since equation (26) implies that  $b_{n,n-1}$  grows more slowly than  $n!$ .) A reasonable description of the dominant growth in the series coefficients is  $h_n(q) \sim n^\alpha(q)$ , with the exponent  $\alpha$  (see the inset of figure 1) taking its maximum value of about 1.2 for  $q \simeq 0.4$ . This of course implies faster-than-exponential growth for the coefficients  $b_{n,m}/n!$ .

Next we examine the behavior of the coefficients in the time series for specific values of the particle density  $p$ . Let

$$\bar{\rho}(t) = \sum_n c_n (-t)^n \quad (28)$$

where

$$c_n \equiv \frac{1}{n!} \sum_{m=0}^{n-1} b_{n,m} p^m. \quad (29)$$

For  $p = 1$  (slightly above the critical value of 0.9493),  $c_n$  is simply the sum of all coefficients at order  $n$ , divided by  $n!$ . The coefficients  $c_n$  again grow faster than exponentially, with  $\ln c_n \sim n^{1.15}$  for  $p = 1$  and  $\sim n^{1.10}$  for  $p = 2$ . (Given the limited number of coefficients, we cannot make very precise estimates of the exponent. The key point is that the growth appears to be faster than exponential.) These results imply that equation (28) is a *divergent series* with zero radius of convergence.

We turn now to an analysis of the series for  $\bar{\rho}(t)$ . As is well known, it is often possible to obtain useful results from divergent series by means of a resummation



technique. In the present case we construct Padé approximants to the time series or to the series obtained via a transformation of variable [13,26–28]. We have examined many transformations, for example

$$y = \frac{1 - e^{-bt}}{b} , \quad (30)$$

$$x = \frac{t}{1 + bt} , \quad (31)$$

$$z = 1 - \frac{1}{(1 + bt)^\gamma} , \quad (32)$$

$$w = 1 - \frac{1}{1 + \ln(1 + bt)} , \quad (33)$$

and

$$v = 1 - \exp \{b[1 - (1 + t)^\gamma]\} . \quad (34)$$

Each transformation maps the interval  $t \geq 0$  to a finite interval, and can be expanded as a power series in  $t$  about  $t = 0$ , with the lowest-order term  $\propto t$ . Each is readily inverted permitting one to express the time  $t$  in powers of the new variable. The slow convergence associated with the power-law or logarithmic forms in the last four expressions is motivated by the numerical finding of slow relaxation in the sandpile model, even far from the critical point [25]. We analyze the transformed series for  $\bar{\rho}$  (or for  $\ln \bar{\rho}$ ) using Padé approximants. The degree of success depends greatly on the range of  $p$  under consideration. (Each transformation includes a free parameter  $b$ , which can be adjusted to optimize the regularity of the result, or to obtain consistency between different approximants. Except where noted, the results do not exhibit much sensitivity to the choice of this parameter.)

For small values of  $p$ , the best results are obtained via Padé approximants to the  $t$ -series *without* any transformation of variable. Figure 2 compares series predictions for  $p = 0.5$  (obtained using the [6,7], [7,8] and [7,9] approximants to the series for  $\bar{\rho}(t)$ ) against the result of a Monte Carlo simulation for a system of 500 sites (for  $p = 0.5$  finite-size effects are negligible at this system size). The [7,8] approximant is reliable for  $t \leq 10$ . (Various other approximants, such as [8,8] and [7,7], are ill-behaved and provide reasonable predictions only for quite short times, typically  $t \leq 2$ .) We have not been able to improve the series prediction for longer times, either by a change of variable or through analysis of  $\ln \bar{\rho}(t)$  or its time derivative. Although some improvement could be expected with longer series, it appears unlikely that the asymptotic decay of  $\bar{\rho}(t)$  in the subcritical regime will be accessible through analysis of an expansion in powers of time.

For larger values of  $p$  the transformation defined in equation (32), using  $\gamma = 1/2$ , is the most useful of those studied. In figure 3 we compare the [8,8] approximant (obtained using  $b = 0.57$ ) with simulation data for  $p = 1$ . The situation is markedly better than for  $p = 1/2$ : the series prediction accompanies the simulation result up to around  $t = 1000$ . It must be noted, however, that the good agreement seen here depends on the choice of the transformation parameter  $b$ . For other values the agreement with simulation is not as good. (A more suitable criterion for choosing  $b$  would be by seeking agreement among various approximants [13]. In the present case this is not possible because the off-diagonal approximants to the  $z$  series are ill-behaved, while the [7,7] approximant behaves very similarly to the [8,8] used here.) Despite the good agreement up to times on the order of 1000, the present series seems incapable of capturing the asymptotic long-time relaxation of  $\bar{\rho}(t)$ , which is non-monotonic, as shown in figure 3.

Remarkably, the reliability of the series improves dramatically at larger values of the particle density  $p$ . Series and simulation results for  $\bar{\rho}(t)$  at  $p = 2$  are compared in figure 4; the maximum relative error is about 0.1%. (The series prediction is generated as for  $p = 1$ , but using  $b = 1.5$  in this case.) The good agreement, moreover, persists at long times, motivating a study of  $\bar{\rho}_\infty \equiv \lim_{t \rightarrow \infty} \bar{\rho}(t)$ , corresponding to the transformed series with  $z = 1$  in equation (32). (We again use the [8,8] approximant to the  $z$ -series.)

The series prediction for  $\bar{\rho}_\infty$  is compared with simulation in figure 5, using parameters  $b = 0.57$  and  $b = 5$ . Excellent agreement is found for  $p \geq 2$ , the relative error being  $\leq 0.2\%$ . The smaller  $b$  value yields better results for  $p \simeq 1$ , whereas slightly better results are obtained for larger  $p$ , using the larger  $b$  value. For  $p \geq 2$  we may claim quantitative accuracy for the series prediction. Nearer the critical point, the agreement appears reasonable (at least on the scale of figure 5), but it is clear that the 16-term series cannot be used to study critical properties. For example, the prediction using  $b = 0.57$  yields a critical value of about 0.906, that is, the extrapolated activity density goes to zero at this  $p$  value. The critical value found in simulations is 0.9493.

In summary, the present series seems quite reliable in the supercritical regime, both at short and at asymptotically long times, whereas its utility in the critical and subcritical regimes is restricted to rather short times. Just above the critical point, rather good predictions are possible for short and intermediate times, but this depends on a judicious choice of the transformation parameter  $b$ .

## VI. DISCUSSION

We develop an algebraic method leading to a time series for the activity density of the stochastic sandpile model introduced in [20]. Determination of the series coefficients depends on evaluation of certain commutators, an algebraic task readily

codified in a computational algorithm. We extend the series for the one-dimensional case to sixteen terms.

Analysis of the series yields disappointing results for the subcritical and critical regimes, but very good predictions in the supercritical region, as judged by comparison with Monte Carlo simulation. At first glance this is surprising, since in the subcritical regime the stationary state is inactive and might be regarded as trivial. Relaxation to this inactive state (and to the active state at or near the critical point  $p_c$ ) is however nontrivial, characterized by stretched exponential, power-law, or other slowly-converging forms [25]. It appears to be very difficult to capture such behavior in the kind of temporal series developed here, which employs a Poissonian initial distribution. The reason is that for smaller values of the particle density ( $p < 2$ , say), the one-site stationary occupation distribution  $P(n)$  is far from Poissonian. As  $p$  increases, the second factorial moment  $\langle n(n-1) \rangle = \rho$  approaches  $p^2$ , as expected for a Poisson distribution. Figure 7 shows that the stationary one-site distribution observed in simulations approaches the corresponding Poisson distribution with the same density  $p$ . (Even for  $p = 8$  there are significant differences between the distributions; but analysis of the third and fourth factorial moments suggests convergence to a Poisson distribution as  $p \rightarrow \infty$ .)

An important open question is whether simply increasing the number of terms would permit one to analyze the small- $p$  regime. The present results suggest that even with 20 or 30 terms this region would remain inaccessible. It appears to be more promising to approach the critical region from above, since for larger particle densities we find good agreement with numerical results. In this context it is interesting that the quality of predictions near the critical point improves greatly on going from 12 to 16 terms. This suggests that further extension of the series, to 20 or more terms, would yield quantitative results for critical properties, through study of relaxational properties at  $p_c$ , or of stationary properties (as in figure 5) as  $p_c$  is approached from above. It would also be of great interest to develop an expansion for a stationary property such as  $\bar{\rho}_\infty$  directly in powers of the particle density  $p$ , but this appears to be much more difficult than deriving an expansion in powers of the time. We leave such investigations, using modified or extended series, as subjects for future work.

## Acknowledgments

We thank the Referee for a suggestion that allowed us to derive an extended series. This work was supported by CNPq, CAPES, and FAPERJ, Brazil.

## REFERENCES

- [1] R. Dickman, A. Vespignani and S. Zapperi, Phys. Rev. E **57**, 5095 (1998).
- [2] J. Marro and R. Dickman *Nonequilibrium Phase Transitions in Lattice Models* (Cambridge University Press, Cambridge, 1999).
- [3] H. Hinrichsen, Adv. Phys. **49**, 815 (2000).
- [4] Various articles on absorbing-state phase transitions are collected in Braz. J. Phys. **30**, (2000).
- [5] A. Vespignani, R. Dickman, M. A. Muñoz, and S. Zapperi, Phys. Rev. E **62** (2000) 4564.
- [6] M. Rossi, R. Pastor-Satorras, and A. Vespignani, Phys. Rev. Lett. **85** (2000) 1803.
- [7] R. Dickman, M. Alava, M. A. Muñoz, J. Peltola, A. Vespignani, and S. Zapperi, Phys. Rev. E **64**, 056104 (2001).
- [8] R. Dickman, T. Tomé, and M. J. de Oliveira, Phys. Rev. E **66**, 016111.
- [9] V. B. Priezzhev, E. V. Ivashkevich, A. M. Povolotsky and C.-K. Hu, Phys. Rev. Lett. **87**, 084301 (2001).
- [10] S. Maslov and Y. C. Zhang, Phys. Rev. Lett. **75**, 1550 (1995).
- [11] G. Baker, Jr., *Quantitative Theory of Critical Phenomena* (Academic Press, New York, 1990).
- [12] R. Dickman, J. Stat. Phys. **55**, 997 (1989).
- [13] I. Jensen and R. Dickman, J. Stat. Phys. **71**, 89 (1993).
- [14] I. Jensen, J. Phys. A **32**, 5233 (1999).
- [15] M. Paczuski, S. Maslov, and P. Bak, Europhys. Lett. **27**, 97 (1994).
- [16] A. Vespignani, R. Dickman, M. A. Muñoz, and S. Zapperi, Phys. Rev. Lett. **81**, 5676 (1998); M. A. Muñoz et al., in *Proceedings of the 6th Granada Seminar on Computational Physics*, J. Marro and P. L. Garrido, Eds., AIP Conference Proceedings v. 574 (2001).
- [17] F. van Wijland, Phys. Rev. Lett. **89**, 190602 (2002).
- [18] S. Lübeck, Phys. Rev. E **64**, 016123 (2001); Phys. Rev. E **66**, 046114 (2002).
- [19] J. Kockelkoren and H. Chaté, preprint: cond-mat/0306039.
- [20] R. Dickman and R. Vidigal, J. Phys. A **35**, 7269 (2002).
- [21] S. S. Manna, J. Phys. A **24**, L363 (1991).
- [22] S. S. Manna, J. Stat. Phys. **59**, 509 (1990).
- [23] R. Dickman, unpublished.
- [24] We are grateful to the Referee for suggesting this approach.
- [25] R. Dickman, Europhys. Lett. **61**, 294 (2003).
- [26] G. Baker, Jr., *Essentials of Padé Approximants* (Academic Press, New York, 1975).
- [27] C. M. Bender and S. A. Orszag, *Advanced Mathematical Methods for Scientists and Engineers* (McGraw-Hill, New York, 1978).
- [28] A. J. Guttmann, in *Phase Transitions and Critical Phenomena*, Vol. 13, C. Domb and J. L. Lebowitz, eds. (Academic Press, New York, 1989).

# TABLES

$n$	$m$	$b_{n,m}$
0	0	1
1	0	1
2	0	1
	1	8
3	0	1
	1	66
	2	80
4	0	1
	1	442
	2	2 076
	3	896
5	0	1
	1	2 842
	2	35 396
	3	52 240
	4	10 752
6	0	1
	1	18 118
	2	516 880
	3	1 737 952
	4	1 187 968
	5	135 168
7	0	1
	1	$\frac{922\,265}{8}$
	2	7 040 282
	3	45 847 512
	4	67 368 480
	5	25 614 368
	6	1 757 184
8	0	1
	1	$\frac{5\,865\,473}{8}$
	2	$\frac{370\,752\,137}{4}$
	3	1 078 168 434
	4	2 871 388 040
	5	2 283 464 832
	6	536 472 640
	7	23 429 120
9	0	1
	1	$\frac{74\,596\,747}{16}$
	2	$\frac{4\,797\,745\,191}{4}$
	3	23 841 662 132
	4	105 679 404 154

	5	147 137 780 760
	6	71 353 965 088
	7	11 072 770 560
	8	318 636 032
10	0	1
	1	<u>474 336 627</u>
	2	<u><sup>16</sup> 123 077 063 429</u>
	3	<u><sup>8</sup> 1 018 938 641 745</u>
	4	<u><sup>2</sup></u>
	5	3 584 915 570 625
	6	7 999 349 570 432
	7	6 656 488 808 368
	8	2 121 777 710 528
	9	227 436 059 136
	10	4 402 970 624
11	0	1
	1	<u>12 064 410 263</u>
	2	<u><sup>64</sup> 3 142 928 518 289</u>
	3	<u><sup>16</sup> 85 419 503 179 415</u>
	4	<u><sup>8</sup></u>
	5	116 020 128 091 449
	6	394 806 480 115 048
	7	514 548 057 479 072
	8	278 154 455 793 952
	9	61 313 513 593 600
	10	4 683 285 856 256
	11	61 641 588 736
12	0	1
	1	<u>76 711 895 439</u>
	2	<u><sup>64</sup> 80 070 040 225 479</u>
	3	<u><sup>32</sup> 1 770 456 755 814 995</u>
	4	<u><sup>8</sup> 14 610 068 149 248 089</u>
	5	<u><sup>4</sup></u>
	6	18 396 700 126 638 476
	7	35 650 110 284 461 928
	8	29 745 976 515 005 712
	9	11 054 665 928 232 448
	10	1 747 506 609 502 464
	11	97 252 577 107 968
	12	872 465 563 648
13	0	1
	1	<u>1 951 093 993 893</u>
	2	<u><sup>256</sup> 2 037 418 656 354 491</u>
	3	<u><sup>64</sup> 72 926 486 692 093 419</u>
	4	<u><sup>16</sup> 905 058 014 398 112 835</u>
	5	<u><sup>8</sup> 1 655 391 460 208 555 433</u>
	6	<u><sup>2</sup></u>
	7	2 309 179 626 832 648 726
	8	2 816 714 002 502 804 952

	8	1 601 275 099 838 022 656
	9	426 223 203 786 122 496
	10	49 655 626 778 919 936
	11	2 046 635 410 882 560
	12	12 463 793 766 400
14	0	1
	1	<u>2 613 736 799 297</u>
	2	<u>11 934 019 637 184 639</u>
	3	<u>711 799 150 376 749 517</u>
	4	<u>53 725 847 102 644 113 051</u>
	5	<u>142 451 880 202 934 178 839</u>
	6	140 971 191 603 315 396 510
	7	243 993 717 303 561 711 492
	8	201 186 302 850 192 322 944
	9	81 746 928 038 823 569 408
	10	16 113 035 142 846 829 824
	11	1 415 730 263 534 155 776
	12	43 811 063 460 921 344
	13	179 478 630 236 160
15	0	1
	1	<u>531 822 407 449 409</u>
	2	<u>606 748 047 325 325 193</u>
	3	<u>116 603 968 592 784 196 927</u>
	4	<u>819 559 563 865 455 675 379</u>
	5	<u>12 371 190 775 573 187 034 899</u>
	6	8 499 377 166 784 889 887 638
	7	20 286 352 375 993 324 998 496
	8	23 298 464 567 721 533 566 328
	9	13 579 307 980 015 469 945 184
	10	4 068 154 005 082 098 401 408
	11	607 110 051 667 479 652 352
	12	40 856 912 571 394 580 480
	13	957 525 442 027 462 656
	14	2 602 440 138 424 320
16	0	1
	1	<u>422 699 161 810 361</u>
	2	<u>61 687 281 835 997 869 817</u>
	3	<u>1 192 545 870 991 479 699 681</u>
	4	<u>12 465 559 773 385 531 628 949</u>
	5	<u>133 184 916 649 036 025 384 179</u>
	6	502 866 857 598 243 404 511 546
	7	1 627 359 034 988 855 536 002 199
	8	2 537 319 446 210 036 202 445 148
	9	2 040 132 355 769 944 077 918 400
	10	872 811 268 389 569 306 302 976

	11	198 169 235 678 101 485 620 992
	12	22 853 161 358 227 259 040 768
	13	1 195 547 596 367 062 589 440
	14	21 401 594 847 260 721 152
	15	37 965 009 078 190 080

Table I. Series coefficients in the expansion of the activity.



## FIGURE CAPTIONS

Figure 1. Function  $h_n(q)$  as defined in text, for  $q = 0.2$  (■);  $q = 0.4$  (●);  $q = 0.6$  (○);  $q = 0.8$  (□). Observe that  $h$  grows faster than linearly for  $q = 0.2, 0.4$ . Inset: growth exponent  $\alpha(q)$  defined via  $h_n(q) \sim n^{\alpha(q)}$ .

Figure 2. Normalized activity  $\bar{\rho} \equiv \rho(t)/p^2$  versus time for  $p = 1/2$  from simulation and various Padé approximants to the times series as indicated.

Figure 3. Normalized activity for  $p = 1$ . Symbols: simulation result; curve: series prediction as described in text.

Figure 4. As in figure 3 for but for  $p = 2$ .

Figure 5. Main graph: limiting activity  $\bar{\rho}_\infty$  versus particle density  $p$ . Points: simulation; solid curve: series prediction using transformation (32) with  $b = 0.57$ , [8,8] Padé approximant; dashed line: same approximant and transformation but using  $b = 5$ . Inset: difference  $\Delta = \bar{\rho}_{\infty,series} - \bar{\rho}_{\infty,sim}$  for  $b = 0.57$  (■) and  $b = 5$  (□).

Figure 6. Single-site occupancy distributions  $P(n)$  obtained in simulation (■) compared with the corresponding Poisson distribution (□). Upper panel:  $p = 1.2$ ; middle:  $p = 3$ ; lower:  $p = 8$ .

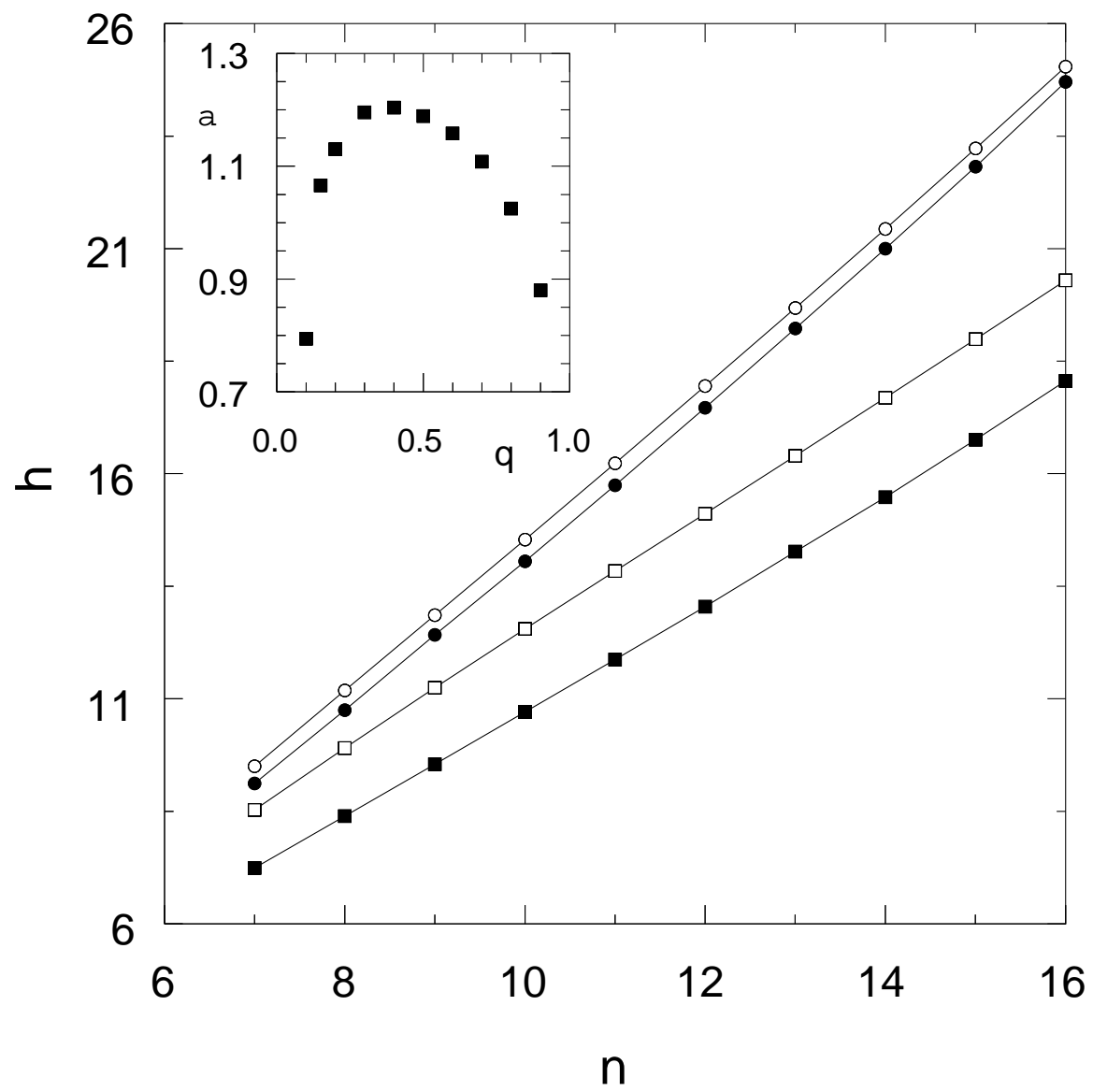


FIG. 1

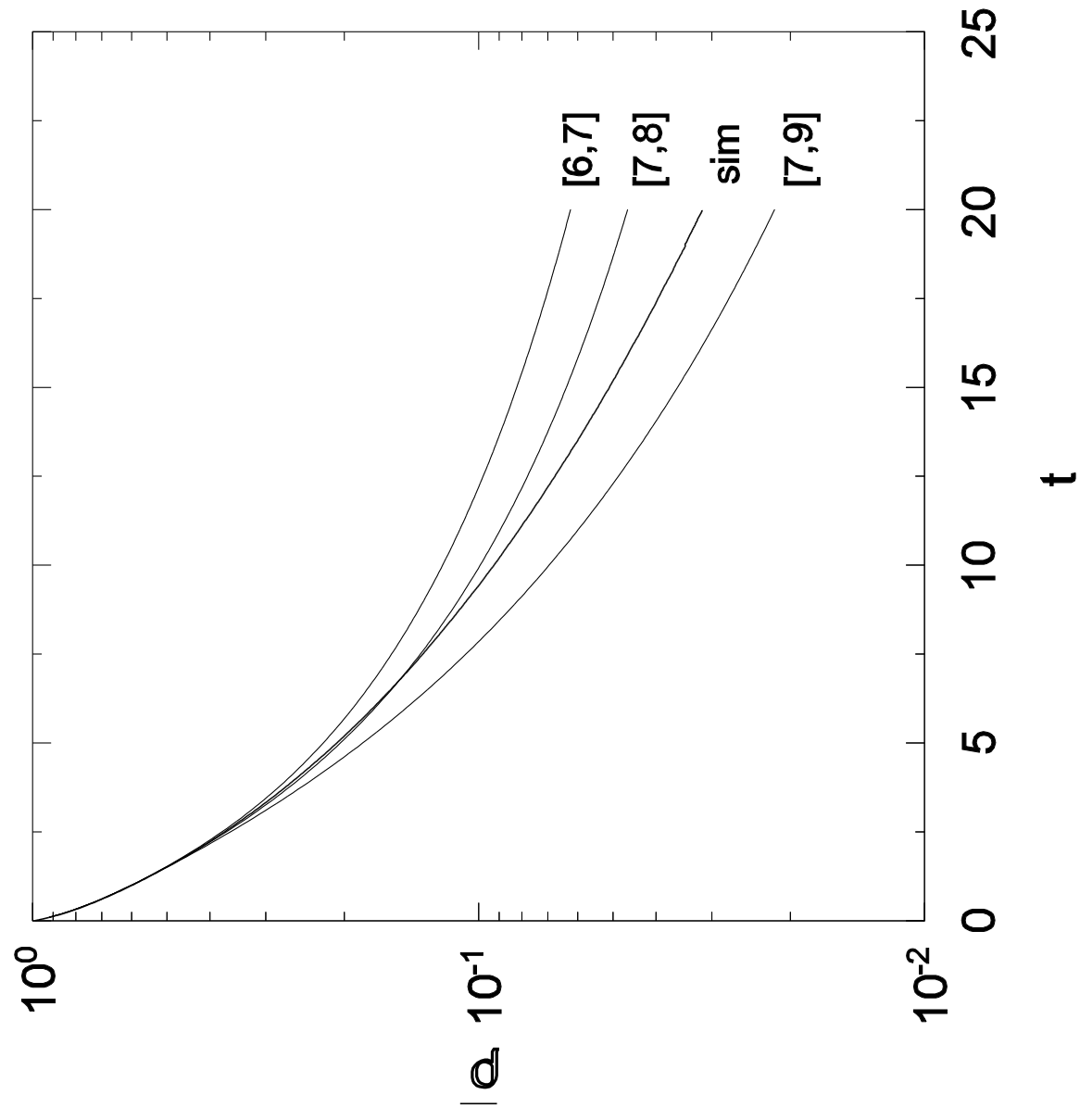


FIG. 2

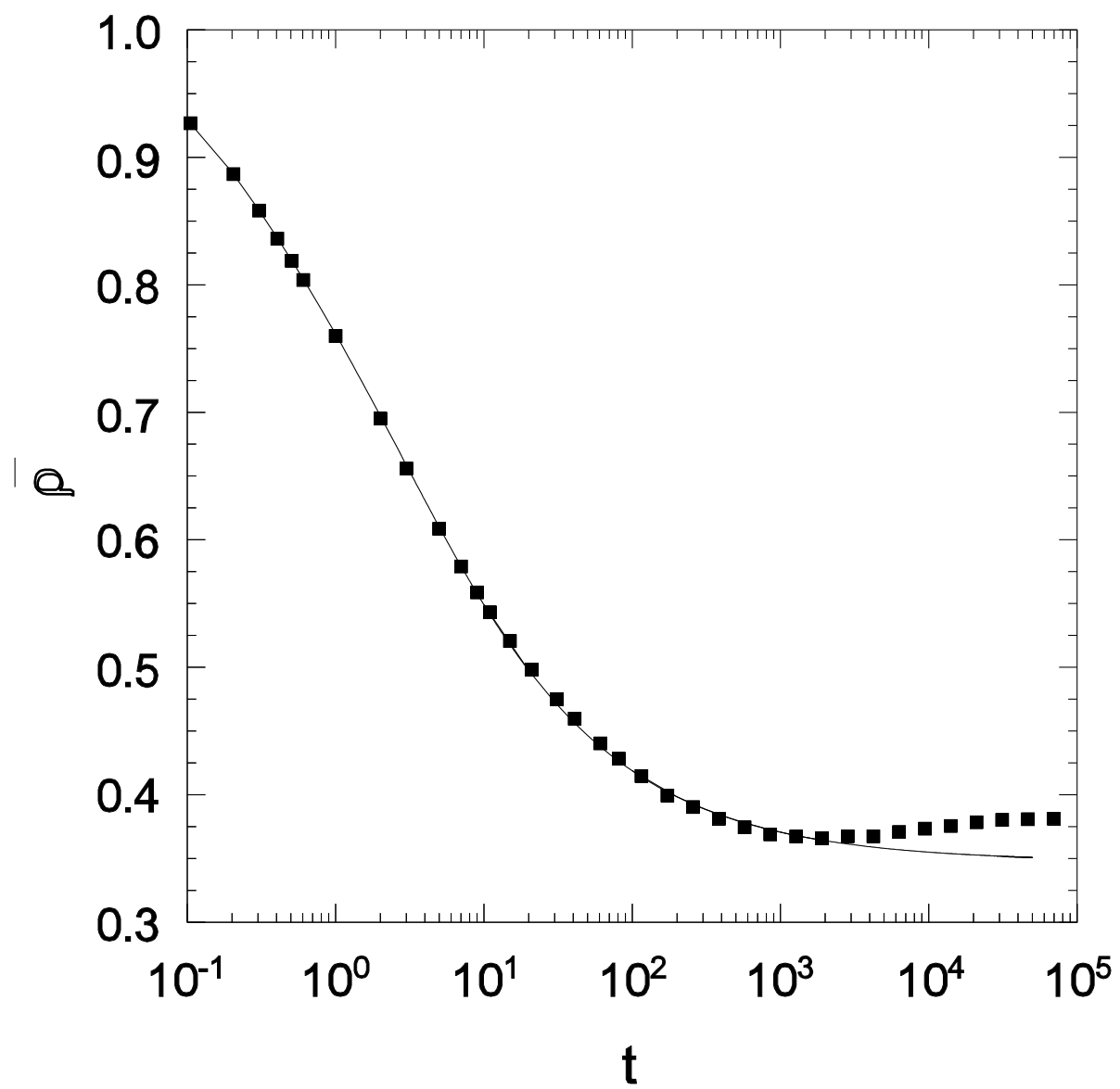


FIG. 3

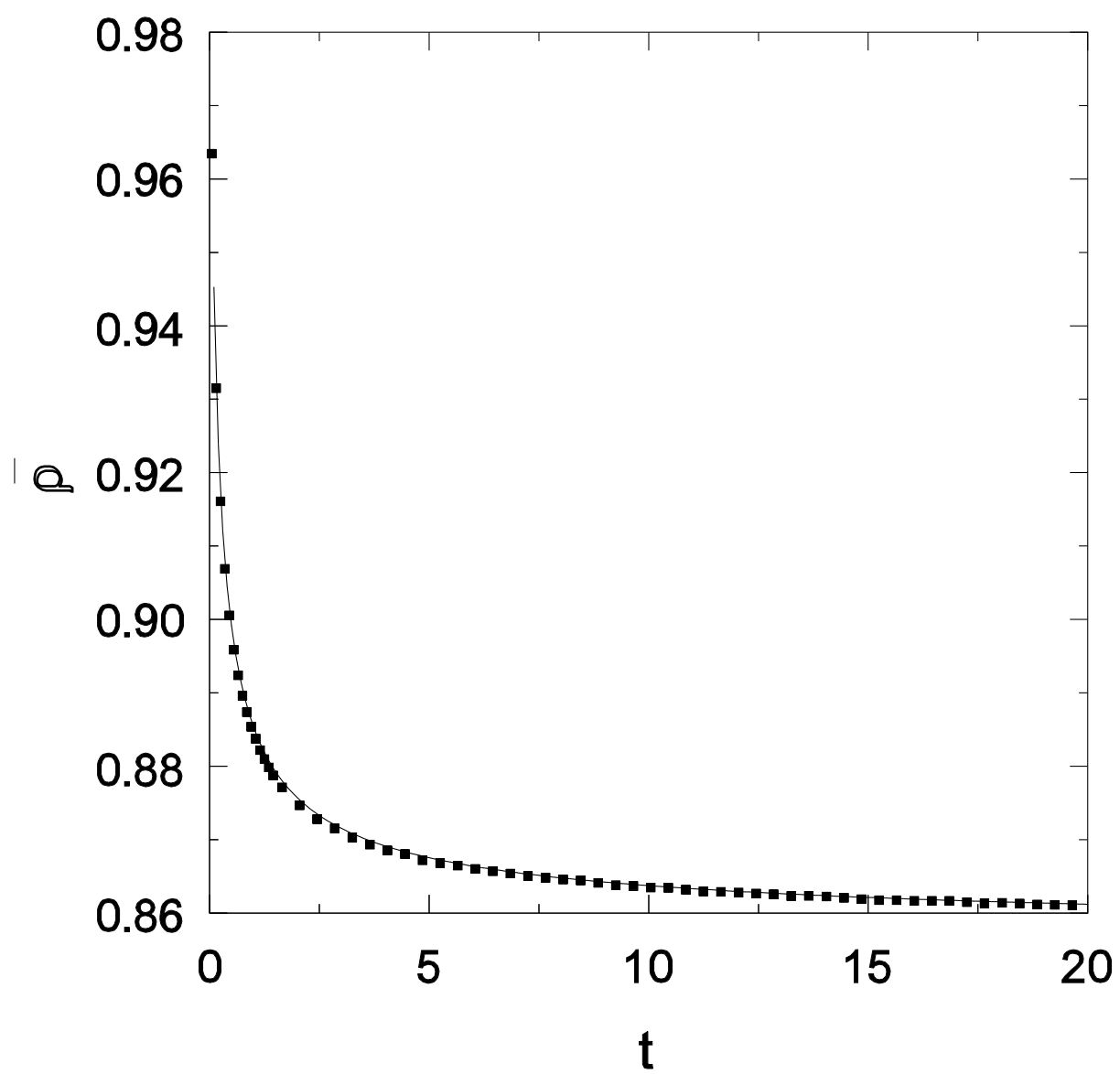


FIG. 4

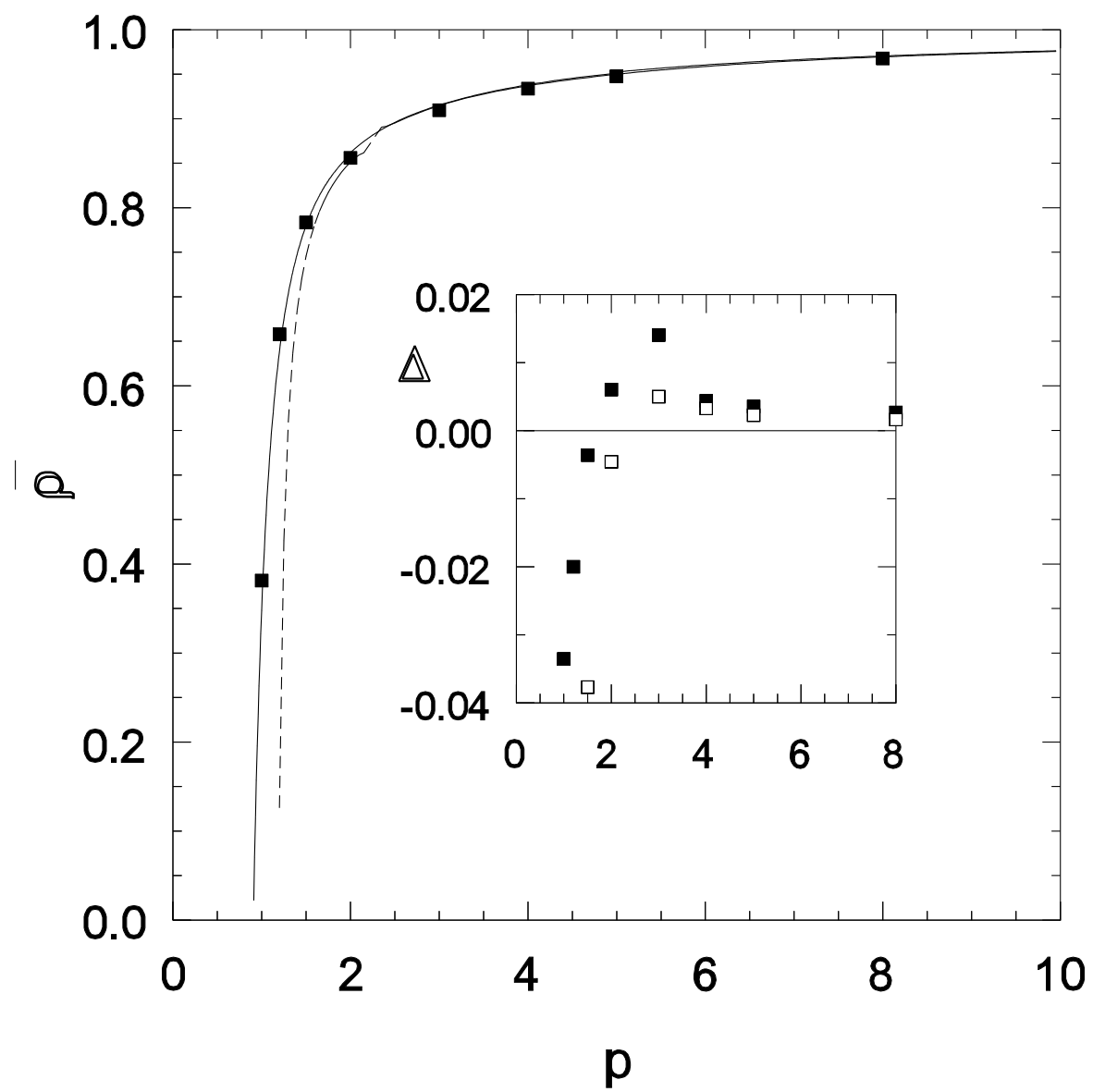


FIG. 5

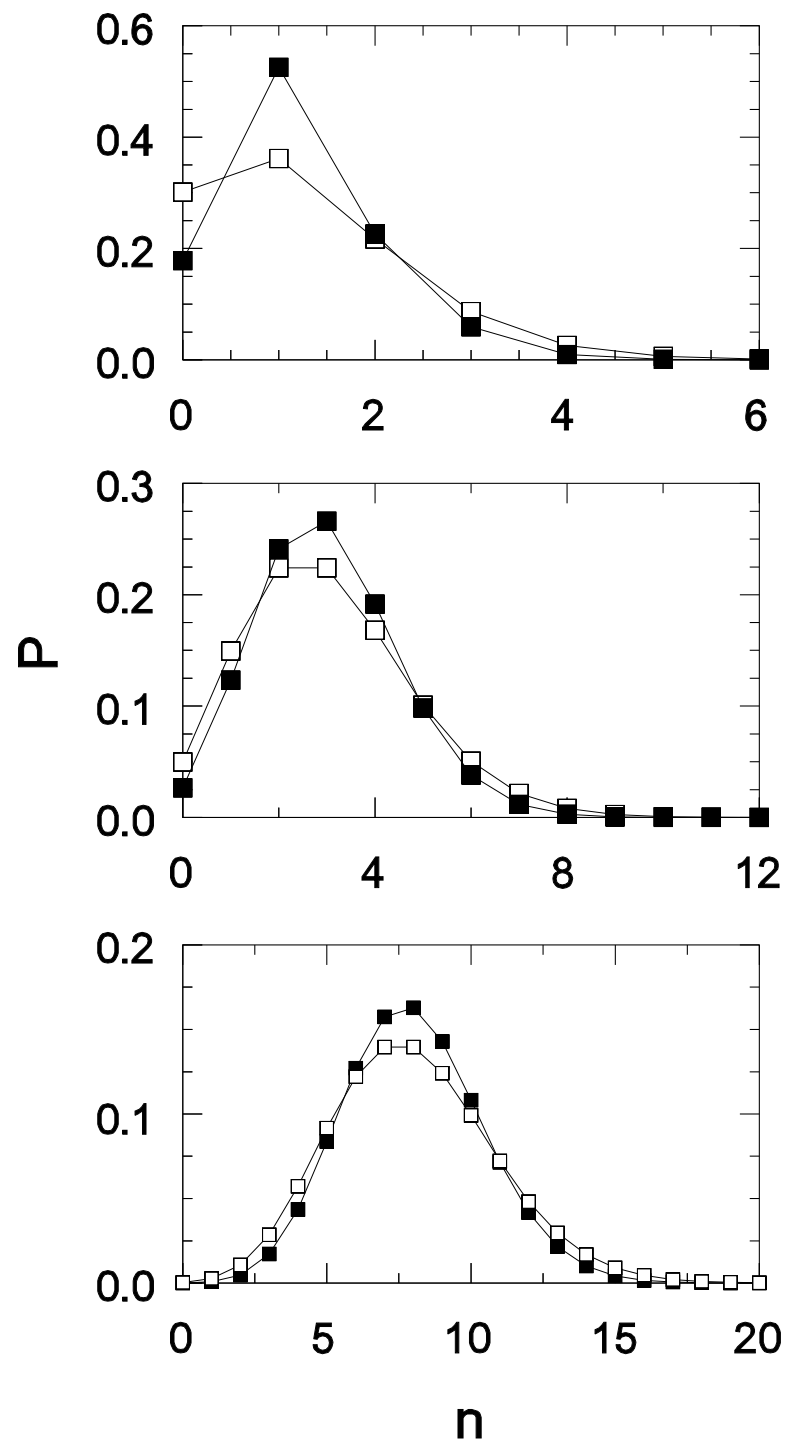


FIG. 6